

# Supplementary Material: Hierarchical fragmentation of regular islands in a discontinuous nontwist map

Matheus Rolim Sales,<sup>1,\*</sup> Michele Mugnaine,<sup>2</sup> Leonardo Costa de Souza,<sup>3,4</sup>  
Iberê Luiz Caldas,<sup>4</sup> Edson Denis Leonel,<sup>1</sup> and José Danilo Szezech Jr.<sup>5,6</sup>

<sup>1</sup>São Paulo State University (UNESP), Institute of Geosciences and Exact Sciences, 13506-900, Rio Claro, SP, Brazil

<sup>2</sup>Lorena School of Engineering (EEL-USP), University of São Paulo, 12602-810, Lorena, SP, Brazil

<sup>3</sup>Department of Physics, Institute for Complex Systems and Mathematical Biology, SUPA, University of Aberdeen, AB24 3UX, Aberdeen, United Kingdom

<sup>4</sup>Institute of Physics, University of São Paulo, 05315-970, São Paulo, SP, Brazil

<sup>5</sup>Graduate Program in Science, State University of Ponta Grossa, 84030-900, Ponta Grossa, PR, Brazil

<sup>6</sup>Department of Mathematics and Statistics, State University of Ponta Grossa, 84030-900, Ponta Grossa, PR, Brazil

In this Supplementary Material, we provide additional phase space plots for different two-dimensional area-preserving maps that are discontinuous on the cylinder for noninteger values of  $m$ . The results further support the interpretation presented in the manuscript, indicating that the fragmentation of regular islands is associated with the interaction between periodic island chains and the discontinuity line generated by the loss of 1-periodicity in the angular variable.

## I. EXTENDED STANDARD NONTWIST MAP

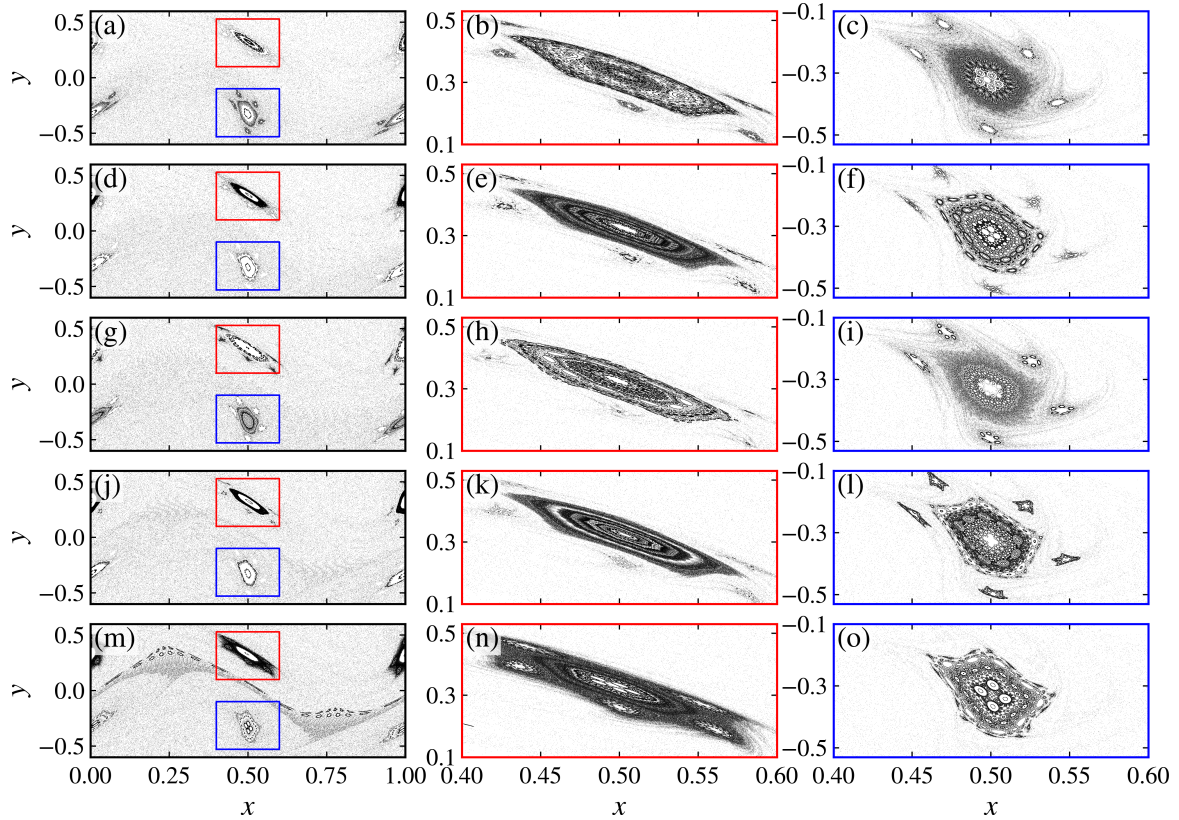


Figure 1. Phase space of the extended standard nontwist map for  $a = 0.56$ ,  $b = 0.56$ ,  $c = 0.005$ , and (a)–(c)  $m = 0.2$ , (d)–(f)  $m = (\sqrt{5}-1)/2$ , (g)–(i)  $m = 1.3$ , (j)–(l)  $m = 2.6$ , and (m)–(o)  $m = 3.8$ . The middle column corresponds to magnifications of the region inside the red dashed rectangle shown in the left column, while the right column corresponds to magnifications of the region inside the blue dashed rectangle shown in the left column.

**Alt text:** Phase-space plots and magnified views of the extended standard nontwist map for several perturbation frequencies. Some regions show smooth nested trajectories surrounding regular islands, while others contain smaller embedded islands, irregular point distributions, and interruptions in the surrounding structures.

\* [rolim.sales.m@gmail.com](mailto:rolim.sales.m@gmail.com)

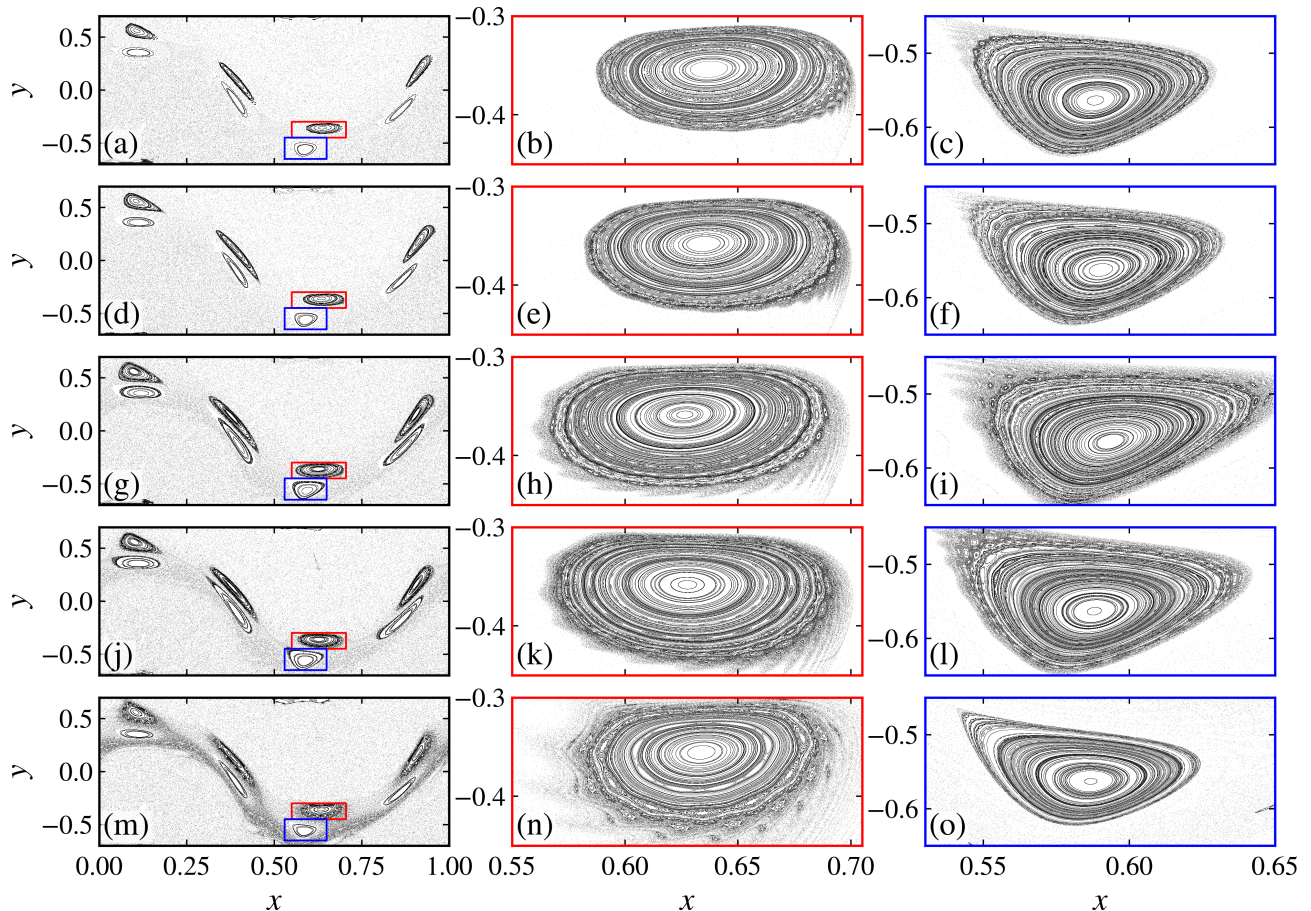


Figure 2. Phase space of the extended standard nontwist map for  $a = 0.285$ ,  $b = 0.72$ ,  $c = 0.005$ , and (a)–(c)  $m = 0.2$ , (d)–(f)  $m = (\sqrt{5}-1)/2$ , (g)–(i)  $m = 1.3$ , (j)–(l)  $m = 2.6$ , and (m)–(o)  $m = 3.8$ . The middle column corresponds to magnifications of the region inside the red dashed rectangle shown in the left column, while the right column corresponds to magnifications of the region inside the blue dashed rectangle shown in the left column.

**Alt text:** Phase-space plots and magnified views of the extended standard nontwist map for a parameter set in which the island chains remain regular. The magnified regions show smooth nested trajectories surrounding the islands, with continuous organization and no visible interruptions in the local structures.

Figure 1 shows the phase space of the extended standard nontwist map for the same parameters ( $a, b, c$ ) used in the main text, but for different values of  $m$ . We consider four rational values of  $m$  and one irrational value [Figs. 1(a)–1(e)]. As expected, changing  $m$  modifies the topology and location of the island chains. Nevertheless, the fragmentation of the regular islands is observed for both rational and irrational values of  $m$ . These phase space plots therefore indicate that the fragmentation phenomenon is not associated with the arithmetic nature of  $m$ .

Figure 2 presents a different configuration, obtained for  $a = 0.285$ ,  $b = 0.72$ , and  $c = 0.005$ , in which none of the period-4 islands from the upper and lower chains intersects the discontinuity line at  $x = 0, 1$ . In contrast to the cases shown in Fig. 1, no fragmentation is observed. This suggests that the fragmentation mechanism is closely related to the interaction between the island chains and the discontinuity line.

## II. STANDARD MAP

To show that the fragmentation phenomenon is not exclusive to nontwist systems, we now consider an extension of the standard map perturbed by two frequencies. The map is defined as

$$\begin{aligned} y_{n+1} &= y_n + \frac{k_1}{2\pi} \sin(2\pi x_n) + \frac{k_2}{2\pi} \sin(2\pi m x_n), \\ x_{n+1} &= x_n + y_{n+1}, \quad (\text{mod } 1), \end{aligned} \quad (1)$$

where  $k_1, k_2 \geq 0$  are perturbation parameters and  $m \in \mathbb{R}$  controls the periodicity of the second perturbation. For noninteger values of  $m$ , the second perturbation is no longer 1-periodic in  $x$ , and therefore the map becomes discontinuous on the cylinder  $\mathbb{T} \times \mathbb{R}$ . As in the extended standard nontwist map,  $k_2$  controls the strength of the additional perturbation.

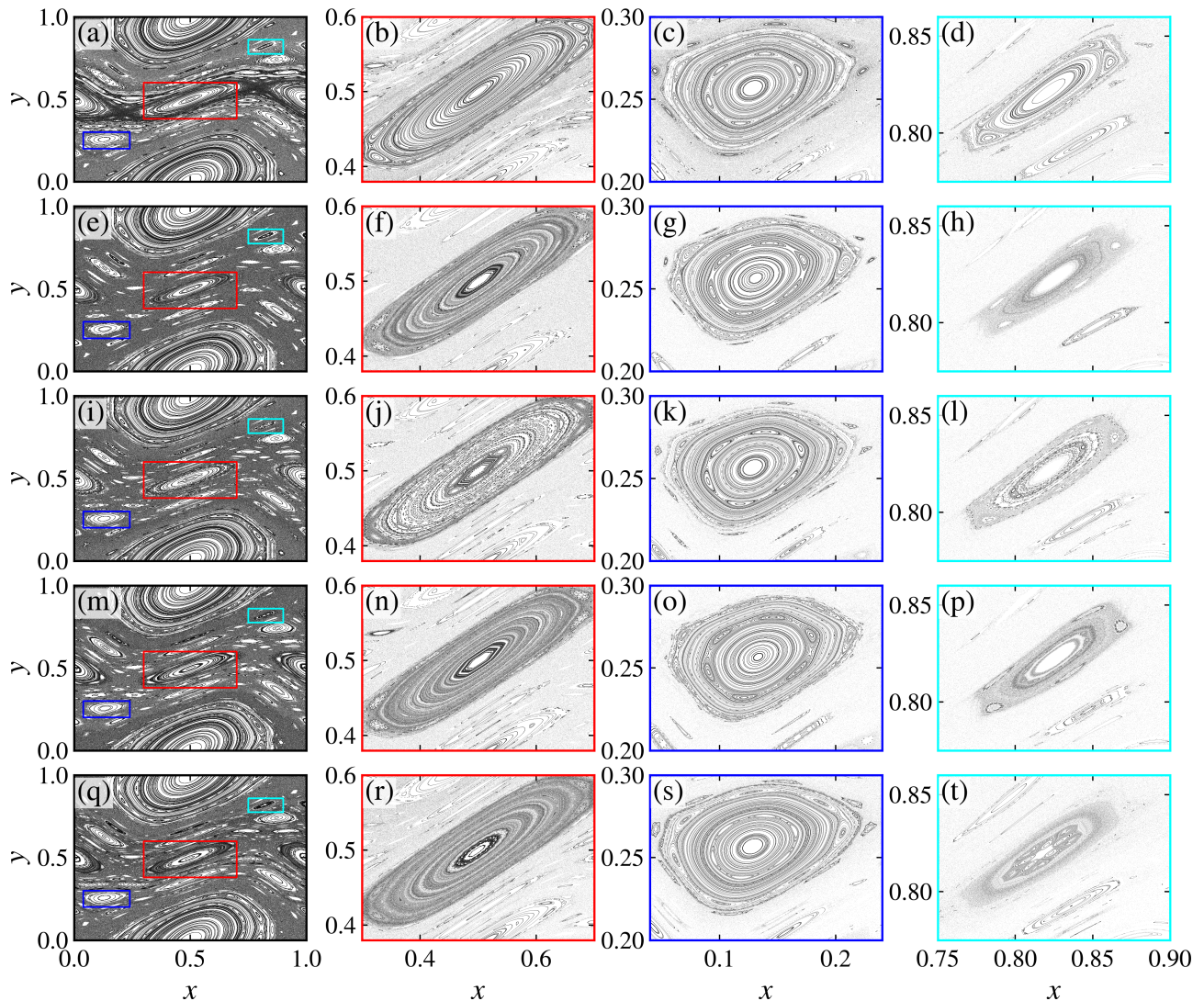


Figure 3. Phase space of the extended standard map [Eq. (1)] for  $k_1 = 1.0$ ,  $k_2 = 0.005$  and (a)–(d)  $m = 0$ , (e)–(h)  $m = (\sqrt{5} - 1)/2$ , (i)–(l)  $m = 1.3$ , (m)–(p)  $m = 2.6$ , and (q)–(t)  $m = 3.8$ . The second, third, and fourth columns show magnifications of the regions enclosed by the red, blue, and cyan dashed rectangles in the first column, respectively.

**Alt text:** Phase-space plots and successive magnifications of the extended standard map for different perturbation frequencies. The unperturbed case shows smooth closed trajectories surrounding regular islands, while other cases contain smaller embedded islands, diffuse scattered regions, and interruptions in the nested structures.

Figures 3 and 4 show the phase space of the extended standard map for  $k_1 = 1.0$  and  $k_1 = 0.75$ , respectively, and  $k_2 = 0.005$ . For  $m = 0$ , the system reduces to the usual standard map and no fragmentation is observed. For noninteger values of  $m$ , fragmentation appears in the island chains intersecting the discontinuity line at  $x = 0, 1$ . This is particularly evident for periodic island chains in which one of the islands is centered on the discontinuity line. For example, in the period-2 chains located at the line  $y = 0$ , one island of the chain is located at  $x = 0, 1$ , and the corresponding regular structure becomes fragmented.

These results indicate that the fragmentation mechanism is geometrical in nature and does not depend on the nontwist character of the map. Instead, it is associated with the interaction between periodic island chains and the discontinuity line generated by the loss of 1-periodicity for noninteger values of  $m$ .

### III. HARPER MAP

As a final example, we consider an extension of the Harper map perturbed by two frequencies. The map is defined as

$$\begin{aligned} y_{n+1} &= y_n - k_1 \sin(2\pi x_n) + k_3 \sin(2\pi m x_n), \\ x_{n+1} &= x_n + k_2 \sin(y_{n+1}) \pmod{1}, \end{aligned} \quad (2)$$

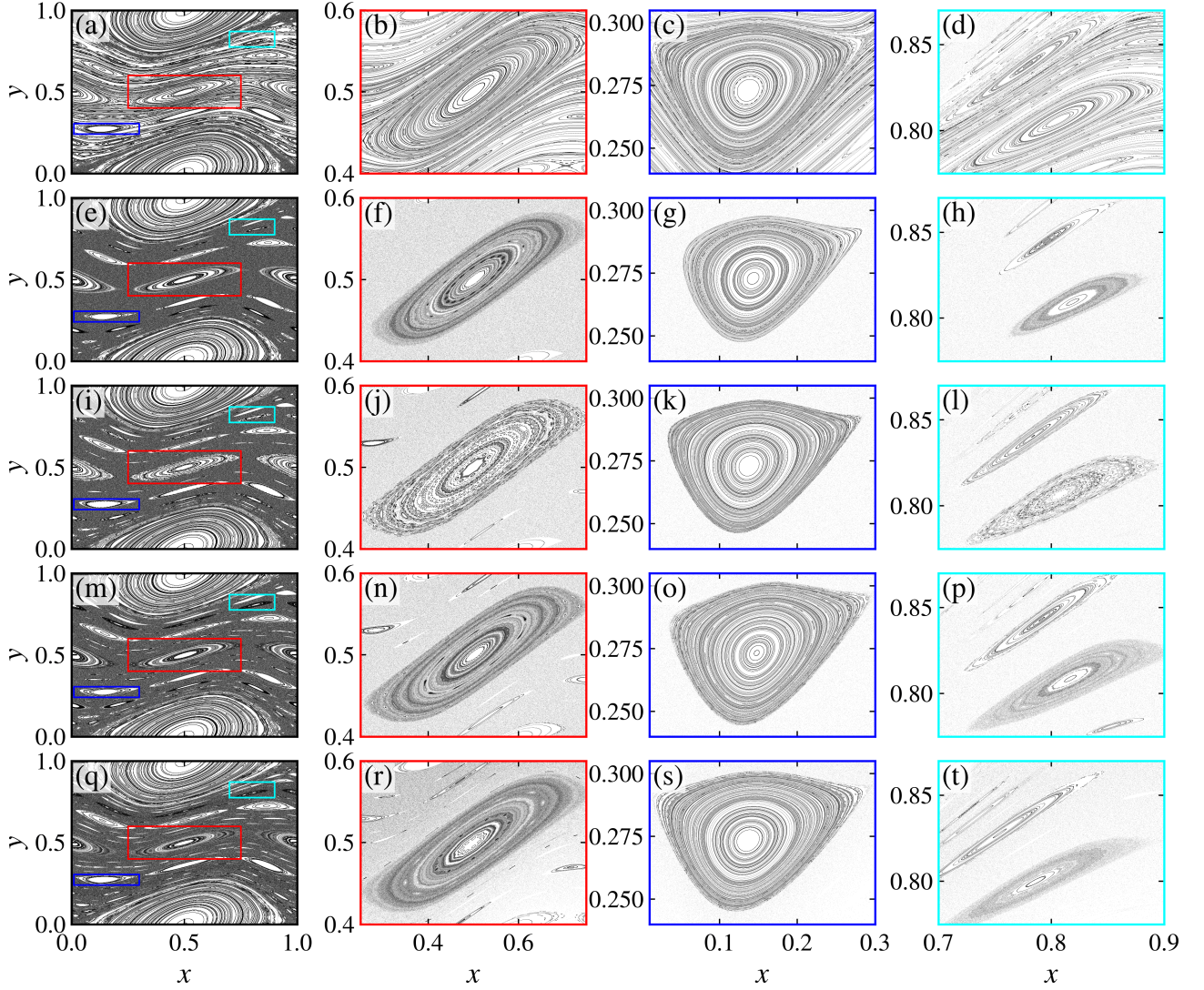


Figure 4. Phase space of the extended standard map [Eq. (1)] for  $k_1 = 0.75$ ,  $k_2 = 0.005$  and (a)–(d)  $m = 0$ , (e)–(h)  $m = (\sqrt{5} - 1)/2$ , (i)–(l)  $m = 1.3$ , (m)–(p)  $m = 2.6$ , and (q)–(t)  $m = 3.8$ . The second, third, and fourth columns show magnifications of the regions enclosed by the red, blue, and cyan dashed rectangles in the first column, respectively.

**Alt text:** Phase-space plots and magnified views of the extended standard map for a second parameter set. Some regions retain smooth closed trajectories around regular islands, whereas others show irregular point distributions, smaller embedded structures, and gaps separating neighboring trajectories.

where  $k_1$ ,  $k_2$ , and  $k_3$  are control parameters and  $m \in \mathbb{R}$  determines the periodicity of the second perturbation. As in the previous systems, noninteger values of  $m$  destroy the 1-periodicity of the map in the angular variable, making the map discontinuous on the cylinder.

Figures 5 and 6 show the phase space of the extended Harper map for two different parameter sets. Figure 5 corresponds to  $k_1 = 0.1$ ,  $k_2 = 0.6$ , and  $k_3 = 0.001$ , while Fig. 6 corresponds to  $k_1 = 0.05$ ,  $k_2 = 0.65$ , and  $k_3 = 0.001$ . The values of  $m$  are the same as those considered for the extended standard map. For  $m = 0$ , the system reduces to the usual Harper map and no fragmentation is observed. For noninteger values of  $m$ , fragmented island structures emerge whenever periodic island chains intersect the discontinuity line at  $x = 0, 1$ . As in the previous examples, island chains with one island centered on the discontinuity line exhibit fragmentation of the corresponding regular structures.

Although the topology of the phase space changes with the control parameters and with the value of  $m$ , the fragmentation mechanism remains qualitatively unchanged. These results reinforce that the fragmentation phenomenon is not specific to a particular map, but rather constitutes a general consequence of the interaction between regular island chains and discontinuity lines generated by the loss of 1-periodicity for noninteger values of  $m$ .

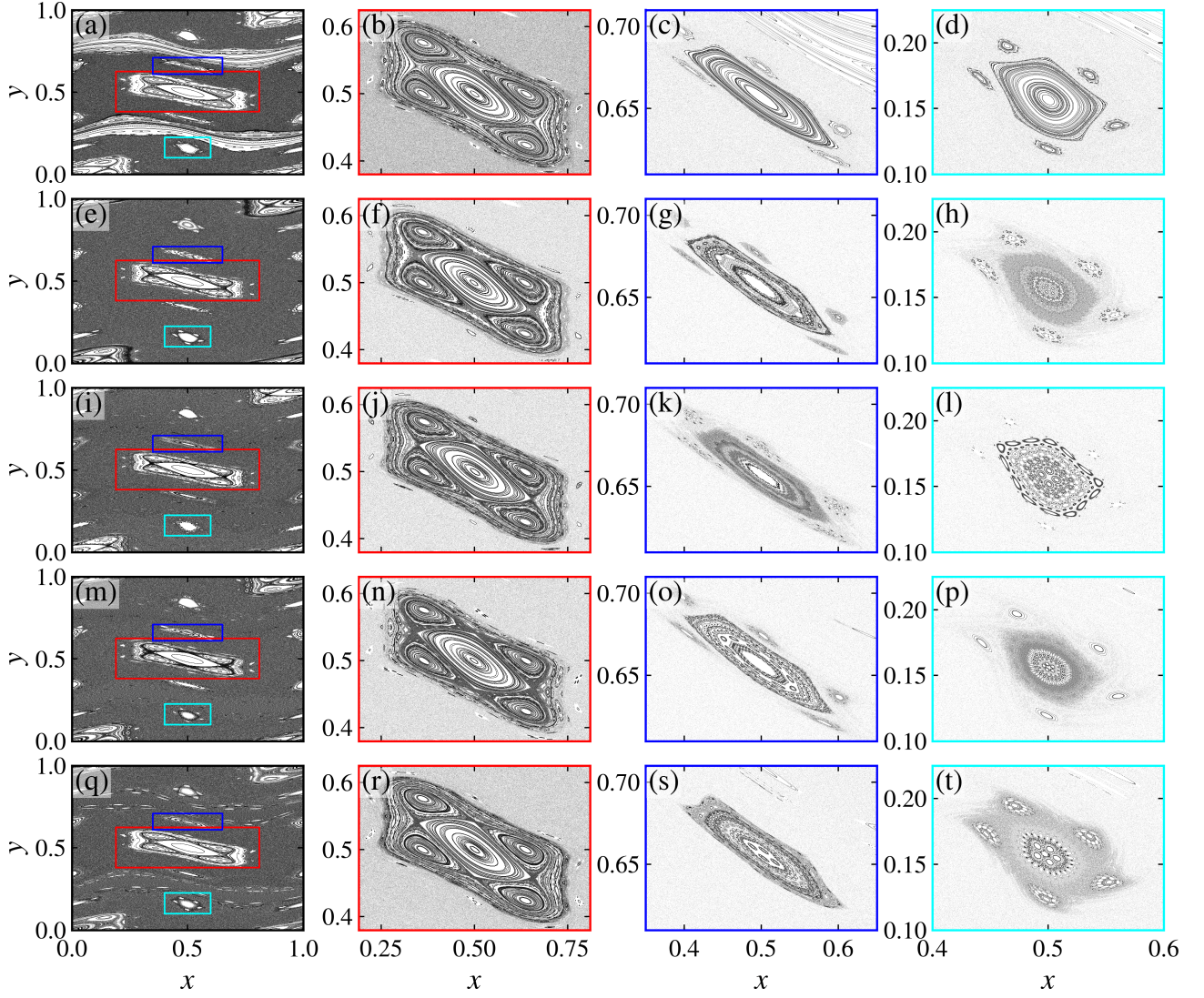


Figure 5. Phase space of the extended Harper map [Eq. (2)] for  $k_1 = 0.1$ ,  $k_2 = 0.6$ ,  $k_3 = 0.001$  and (a)–(d)  $m = 0$ , (e)–(h)  $m = (\sqrt{5}-1)/2$ , (i)–(l)  $m = 1.3$ , (m)–(p)  $m = 2.6$ , and (q)–(t)  $m = 3.8$ . The second, third, and fourth columns show magnifications of the regions enclosed by the red, blue, and cyan dashed rectangles in the first column, respectively.

**Alt text:** Phase-space plots and magnified views of the extended Harper map for several perturbation frequencies. Regular islands are surrounded by smooth nested trajectories in some regions, while others contain smaller internal structures, irregular point distributions, and interruptions in the surrounding organization.

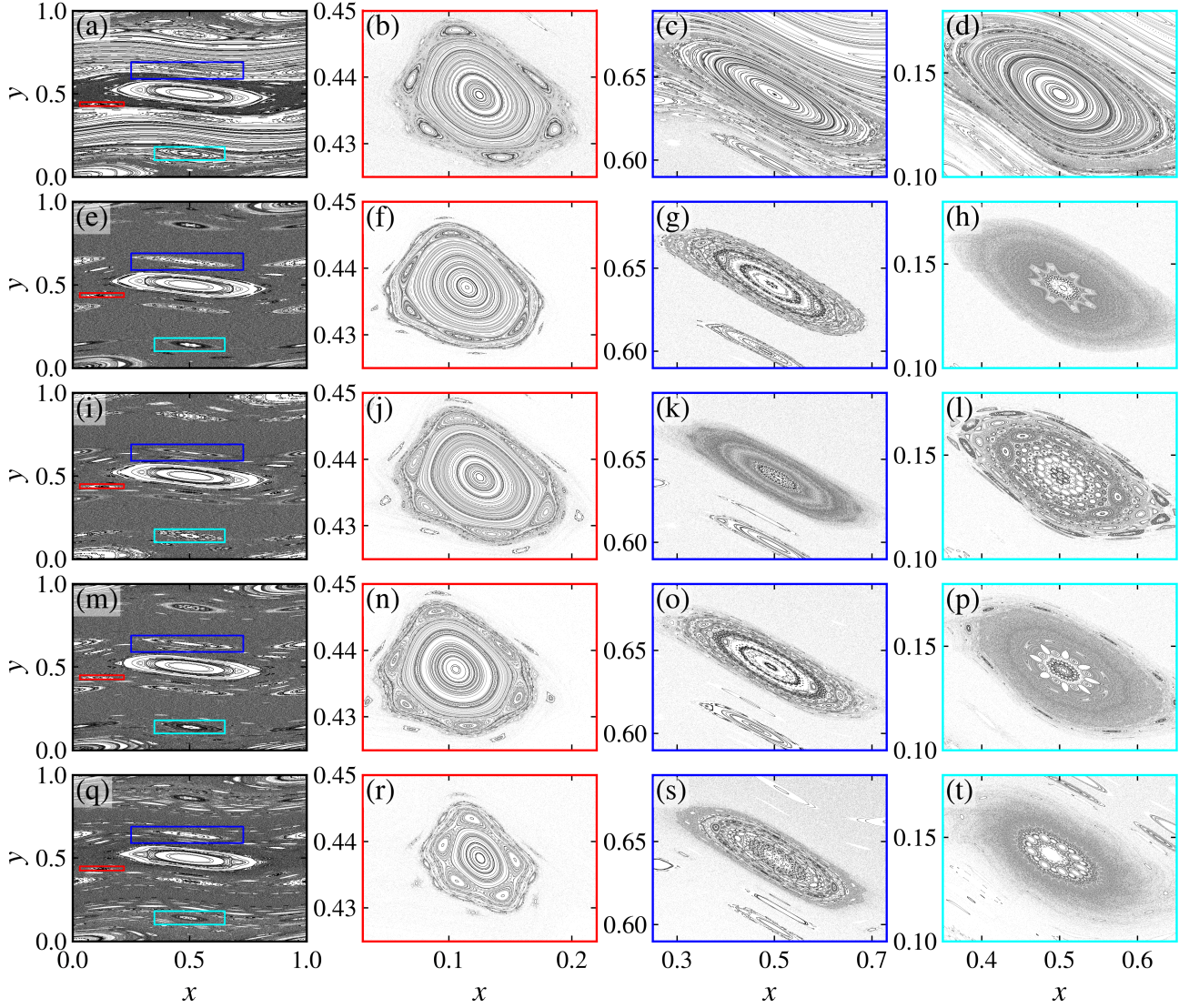


Figure 6. Phase space of the extended Harper map [Eq. (2)] for  $k_1 = 0.05$ ,  $k_2 = 0.65$ ,  $k_3 = 0.001$  and (a)–(d)  $m = 0$ , (e)–(h)  $m = (\sqrt{5} - 1)/2$ , (i)–(l)  $m = 1.3$ , (m)–(p)  $m = 2.6$ , and (q)–(t)  $m = 3.8$ . The second, third, and fourth columns show magnifications of the regions enclosed by the red, blue, and cyan dashed rectangles in the first column, respectively.

**Alt text:** Phase-space plots and magnified views of the extended Harper map for a second parameter configuration. Some island regions remain organized by smooth closed trajectories, while others exhibit smaller embedded structures, scattered regions, and discontinuities in the local arrangement of trajectories.